Ocean Engineering 266 (2022) 113157

Contents lists available at ScienceDirect

Ocean Engineering

journal homepage: www.elsevier.com/locate/oceaneng

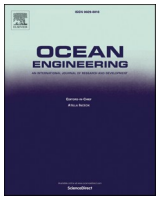

Internal strength characterization of geotextile tube using miniature cone

Dong-Ju Kim [a], Sang-Chul Kim [b], Jong-Sub Lee [a], Yong-Hoon Byun [b,*], Byung-Yoon Kang [c]

[a] School of Civil, Environmental and Architectural Engineering, Korea University, 145, Anam-ro, Seongbuk-gu, Seoul, 02841, South Korea
[b] School of Agricultural Civil & Bio-Industrial Engineering, Kyungpook National University, 80 Daehak-ro, Buk-gu, Daegu, 41566, South Korea
[c] Rural Research Institute, Korea Rural Community Corporation, 870, Haean-ro, Sangnok-gu, Ansan-si, Gyeonggi-do, 15634, South Korea

ARTICLE INFO

Keywords:
Coastal protection
Cone penetration
Geotextile tube
Miniature cone
Internal strength

ABSTRACT

Geotextile tubes are widely used in coastal protection and beach restoration. The objective of this study is to evaluate the internal shear strength of geotextile tubes using a miniature cone in a small-scale model test. Sandy soils with different particle size distributions are used as fill materials in the geotextile tubes. Each fill material with high water content is injected into the geotextile tube using a sand pump. After injecting the fill material, cone penetration tests are conducted using a miniature cone to characterize the internal strength profile of the geotextile tube. The experimental results indicate that fill materials with fines content have smaller cone tip resistances than those without. Moreover, the cone tip resistances near the inlet of the geotextile tube are smaller than those far from the inlet in the longitudinal direction. The strength characterization approach using a miniature cone may be promising for evaluating the internal stability of geotextile tubes.

1. Introduction

Geotextile tubes, which are tubular containers formed on-site, have been widely used in many hydraulic and marine applications, such as coastal protection and beach restoration, as shown in Fig. 1 (Alvarez et al., 2007; Das Neves et al., 2015; Man et al., 2018; Oh and Shin, 2006; Shin and Oh, 2007). Geotextile tubes are permeable materials with apparent opening sizes that can be filled hydraulically or mechanically. Soils dredged on-site with a high water content are typically used to hydraulically fill the geotextile tubes. Owing to the permeability of geotextiles, geotextile tubes can drain the water and retain the soil particles of the slurry used as the fill material. Geotextile tubes are constructed with various diameters ranging from one to several meters and theoretically infinite lengths, depending on the site conditions (Cantré, 2002). Geotextile tubes are cost-effective and easy to transport and install in the field (Fowler et al., 1996; Kim and Dinoy, 2021; Palmeira et al., 2019).

Laboratory and full-scale tests have been conducted to evaluate the field performance and behavior of geotextile tubes. Moo-Young and Tucker (2002) defined filtration and dewatering efficiency according to geotextile tubes and fill material. Koerner and Koerner (2006) conducted a hanging bag test to evaluate the permeability of geotextile tubes at various sites. Yee and Lawson (2012) suggested a correlation among the dewatering process, tube volume, and solid concentration based on full-scale field tests. The internal strength of a geotextile tube is influenced by the type of fill material. As the internal strength of the geotextile tube increases, it becomes a stable structure (Lawson, 2008). Especially for stacked geotextile tubes, the structural stability of the tubes may be affected by the internal shear strength of the geotextile tube. Shin et al. (2016) investigated the behavior of stacked geotextile tubes through on-site monitoring, whereas Kim et al. (2022) used digital image correlation.

To determine the internal strength of the fill material, vane shear and cone penetration tests have been conducted in previous studies (Shin and Oh, 2003; Van Steeg and Vastenburg, 2010; Koh et al., 2020; Karadoğan et al., 2022). However, the vane shear test is restricted to soft soils, and it is difficult to continuously measure the soil strength profile with depth (Hirst et al., 1972). Furthermore, the cone penetration tests can only provide a low-resolution strength profile because of the large diameter of the cone (Lee et al., 2009). Thus, high-resolution strength profile characterization is still required for the filling materials in geotextile tubes.

Cone penetration tests have been widely performed for in situ subsurface characterization. A standard cone penetrometer with a diameter of 35.7 mm can provide soil strength profiles. To improve the sensitivity of the cone tip resistance, various types of smaller-diameter cones have been developed in previous studies (Byun et al., 2013; Kim et al., 2010; Lee et al., 2009; Tumay and Kurup, 2001; Yoon and Lee, 2012; Yoon

* Corresponding author.
E-mail address: yhbyun@knu.ac.kr (Y.-H. Byun).

https://doi.org/10.1016/j.oceaneng.2022.113157
Received 24 July 2022; Received in revised form 5 November 2022; Accepted 12 November 2022
Available online 18 November 2022

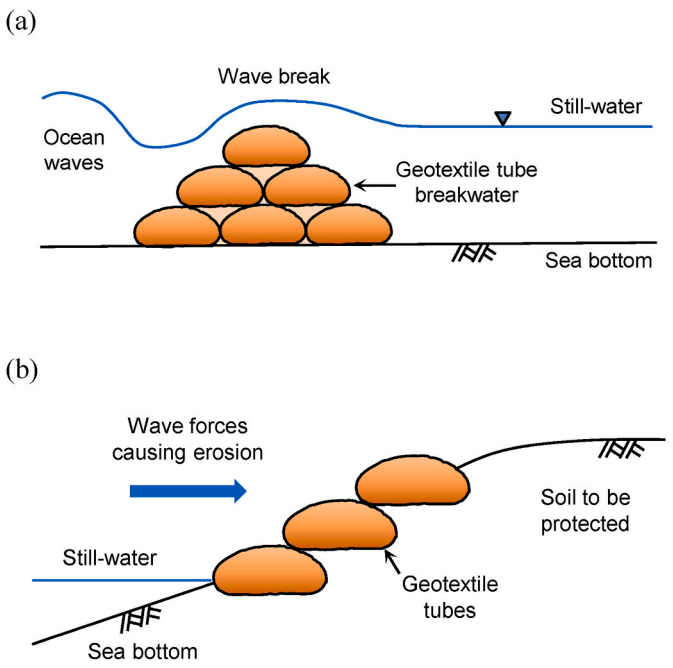

Fig. 1. Schematic drawing of geotextile tubes for coastal protection: (a) submerged breakwater; (b) revetments.

et al., 2015). To detect the cone penetration resistance, a Wheatstone bridge circuit configured with four strain gauges is typically used to amplify the output voltage. Lee et al. (2009) suggested a miniature cone using a half-bridge circuit. Because the cone resistance based on a half-bridge circuit can be affected by temperature changes, a miniature cone configured with a full-bridge circuit was designed to produce more stable and reliable resistance values (Yoon and Lee, 2012). A miniature cone based on fiber-optic sensors was developed by Kim et al. (2010). However, the high cost of the interrogator used for fiber-optic sensors has led to the limited availability/use of such miniature cones. Small-sized cone penetrometers are suitable for minimizing soil disturbance during penetration and for detecting thin soil layers. Considering that the fill material in geotextile tubes is only confined by flexible geotextiles, a miniature cone penetrometer is required to evaluate the internal shear strength of geotextile tubes and to minimize the boundary effect on the cone resistance.

The purpose of this study is to evaluate the internal shear strength of geotextile tubes using a miniature cone in a small-scale model test. This paper introduces the physical properties of the geotextile tubes and fill materials used in this study and explains the experimental setup and procedure for the model tests. Finally, the strength characterization of the geotextile tubes filled with four different materials is discussed.

2. Materials and methods

Four sandy soils were used to investigate the effect of particle size distribution of fill materials on the internal strength of geotextile tubes. The particle size distribution of the sandy soils obtained from a sieve analysis is shown in Fig. 2(a). The index properties of the soils are summarized in Table 1. The mean diameters (D_{50}) of the four sandy soils were 0.25, 2.92, 0.57, and 0.31 mm, which were classified based on the Unified Soil Classification System (USCS), as SP, SW, SP-SM, and SM, respectively. The sandy soils with a water content of 300% were prepared for injection into a geotextile tube.

The geotextile tube used in this study, with a theoretical diameter of 153 mm, was composed of woven geotextiles fabricated using a polyester fabric. The tensile strengths of the woven geotextile were 208 kN/m and 252 kN/m in the machine and cross-machine directions,

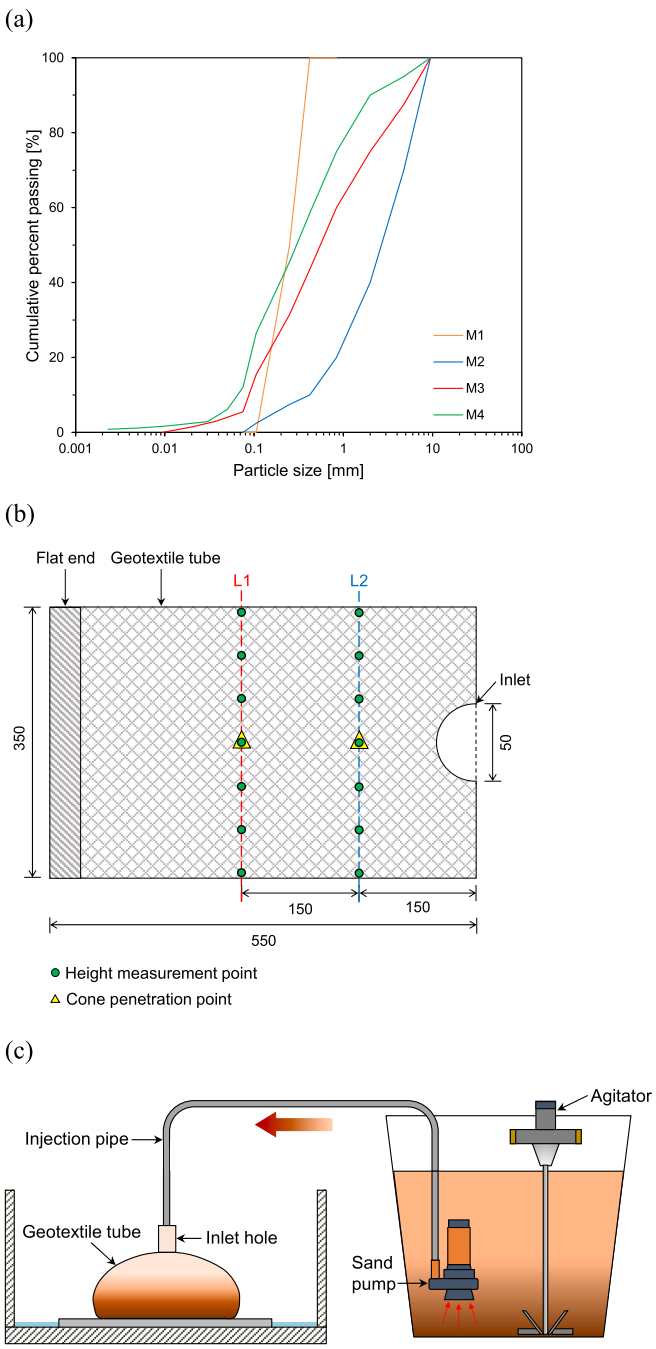

Fig. 2. Geotextile tube with fill material: (a) particle size distribution of sandy soils; (b) one-half geotextile tube in plan view; (c) filling and mixing apparatus. The numbers are in the unit of mm.

respectively. The strains at the maximum load of the geotextile were 9.3% and 11.2% in the machine and cross-machine directions, respectively. According to ISO 12956 (1999), the characteristic opening size (O_{95}) of the geotextile is 219 μm. For the model test, the cylindrical geotextile tubes were sewn with a seam strength of 150 kN/m. Fig. 2(b) shows one-half of the geotextile tubes with a length of 1100 mm and a width of 350 mm. The geotextile tube includes flat ends owing to the sewing at the top and bottom. To inject the fill material, the geotextile tube had an inlet hole with a diameter of 50 mm in the middle. The measurement points for the height of the geotextile tube were located 300 mm and 150 mm from the inlet of the geotextile tube and named L1 and L2, respectively. Measurement lines L1 and L2 were selected to minimize the boundary effect on the shape of the geotextile tube because

Table 1
Index properties of fill material used in this study.

Fill material	D_{10} [mm]	D_{30} [mm]	D_{50} [mm]	D_{60} [mm]	C_u	C_c	#200 [%]	PI [%]	LL [%]	PL [%]	G_s	USCS
M1	0.14	0.19	0.25	0.28	2.1	0.96	0	16.7	19.5	2.8	2.67	SP
M2	0.42	1.42	2.92	3.83	9.11	1.25	0	14.7	18.3	3.6	2.65	SW
M3	0.091	0.22	0.57	0.84	9.23	0.63	5	11.5	17	5.5	2.88	SP-SM
M4	0.063	0.13	0.31	0.42	6.67	0.64	12	11.5	21.8	10.3	2.88	SM

D_{10} = 10% cumulative passing, D_{30} = 30% cumulative passing, D_{50} = 50% cumulative passing, D_{60} = 60% cumulative passing, C_u = coefficient of uniformity, C_c = coefficient of curvature, #200 = percent passing No.200 sieve, PI = plasticity index, LL = liquid limit, PL = plastic limit, G_s = specific gravity.

of the sewn sections at the edge that resulted in the flat ends of the geotextile tube. The measurement points were placed at 70 mm intervals along the measurement lines. To transfer the fill material, an injection pipe connected to the pump outlet was extended to the inlet hole of the geotextile tube, as shown in Fig. 2(c). A Y-shaped pipe splitter was installed in the inlet hole to fill the geotextile tube uniformly. The sandy soils were injected into the geotextile tubes using a sand pump. During the injection, the fill material was continuously mixed using an agitator to prevent sinkage and flocculation of soil particles over time. Using the sand pump, the geotextile tube was filled at a flow rate of 200 L/min. The filling process was completed when the geotextile tube was filled with fill materials. As the geotextile tube dewatered over time, its height decreased, and its shape changed. Consequently, the heights of the geotextile tubes at the two lines were measured every 4 min. The time required to dewater the geotextile tube after injecting the fill material was measured at several filling stages. The filling and dewatering of the geotextile tube were repeated.

The measured dewatering time for the entire filling stage is shown in Fig. 3(a). M2 had the shortest dewatering time, whereas M4 had the longest dewatering time. Considering the effective sizes (D_{10}) of the four soils, the dewatering time increased with smaller effective sizes. Notably, M2 and M4 exhibited the largest and smallest effective sizes, respectively. Previous studies have reported that a fill material with fines content forms a filter cake inside the geotextile tube, which leads to a low shear strength (Khachan and Bhatia, 2016; McCafferty and Hsuan, 2020). Considering the dewatering time for each fill material, the filter cakes could have formed in M3 and M4. Fig. 3(b) shows that the heights of the geotextile tubes measured at four different locations in L1 varied with the horizontal location and sandy soil type. Regardless of the horizontal location, M2 and M4 exhibited the highest and lowest height, respectively. These results are consistent with those of previous studies (Cho et al., 2008; Shin and Oh, 2003), which demonstrated that dredged sand with lower fines content showed higher geotextile tube heights than silty sand. For the geotextile tubes filled with the four soils, the average heights at L1 were greater than those at L2 because of the Y-shaped pipe splitter. Previous studies have reported that the height increases with increasing distance from the inlet. (Kim et al., 2016a). After filling and dewatering of the geotextile tube, cone penetration tests were conducted in the middle of each measurement line using a miniature cone to evaluate the strength profile of the fill material.

The weight of the geotextile tube was measured after the completion of the cone penetration test. In this study, the volumes of the geotextile tubes were estimated using the equation proposed by Leshchinsky et al. (1996). The unit weights estimated for the four fill materials are presented in Table 2. The unit weight values estimated in this study are similar to those of the fill materials reported by Kim et al. (2016b). The fill material used by Kim et al. (2016b) was a silty sand with 150%–170% water content.

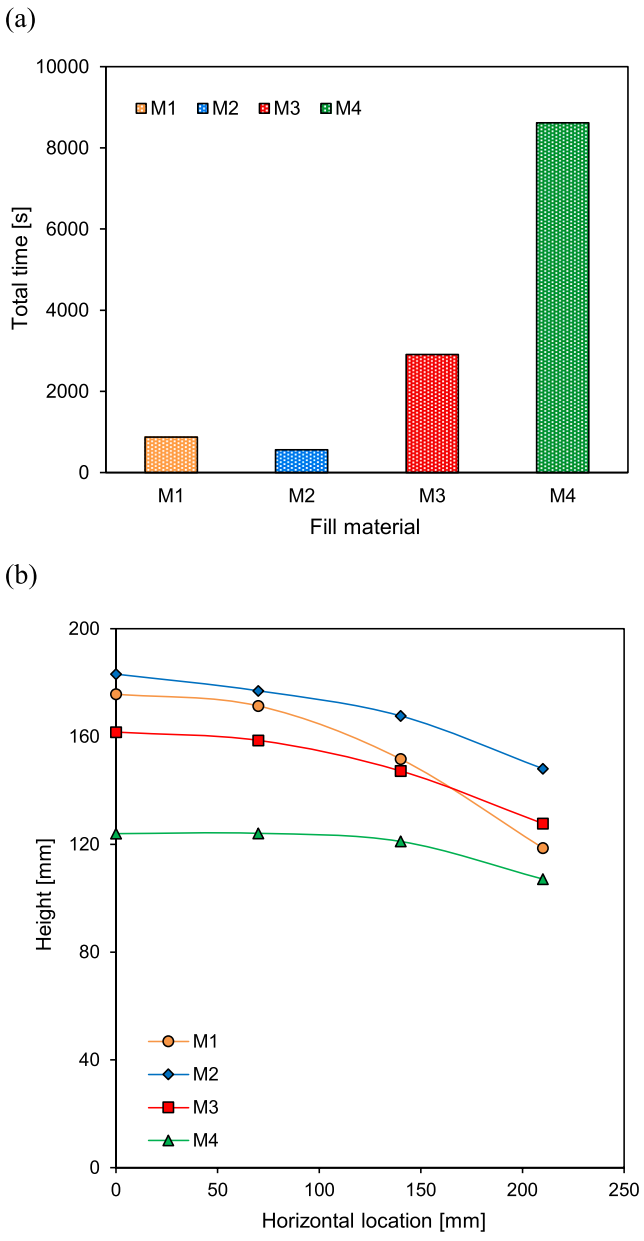

Fig. 3. Behavior of geotextile tubes with different fill materials: (a) dewatering time; (b) heights of half cross-section along horizontal location.

3. Results and discussion

A miniature cone penetrometer system was used to evaluate the internal strength profile of the geotextile tube filled with sandy soils, as shown in Fig. 4. The miniature cone had a tip diameter of 10 mm, apex angle of 60°, and cross-sectional area of 78 mm^2. A full-bridge circuit configured with four strain gauges was used to measure and amplify the change in electrical resistance induced by the axial load and temperature. Two active strain gauges were attached above the cone tip, whereas the other two gauges were installed as dummies above the rod connection. Owing to the selected gauge arrangement and circuit, the effects of bending and temperature on the estimated cone tip resistance

Table 2
Moist unit weights of geotextile tubes in this study.

Fill material	Moist unit weight [kN/m^3]
M1	13.4
M2	13.0
M3	13.8
M4	16.1

can be minimized. The miniature cone was connected to a data logger, and the cone tip resistance was recorded automatically. Cone penetration tests using the miniature cone were conducted on the filled geotextile tube to determine the profiles of the cone tip resistance in the middle of L1 and L2. In this study, the ratio of the distance at the penetration point from the nearest geotextile tube boundary to the cone diameter was 17.5, which is greater than the required ratio of the container side boundary to the cone diameter reported by Bolton et al. (1999). Yang (2006) reported that the influence zone below the cone tip in silty sand corresponds to 1.5 to 3 times the cone tip diameter. Considering the influence zone below the cone tip, a final penetration depth of 80 mm was set for all fill materials. Therefore, the side boundary effect in the geotextile tube was disregarded in the cone penetration tests using the miniature cone. The miniature cone was pushed down at a penetration rate of 1 mm/s using an electric motor.

The cone tip resistances for the four different fill materials were obtained using a miniature cone in the cone penetration tests. Fig. 5 shows the variance in the cone tip resistances for the four fill materials with penetration depth. The cone tip resistances increased with penetration depth, and the cone tip resistances at L1 were greater than those at L2. Previous studies have shown that cone tip resistance increases with penetration depth, regardless of the fill material (Van Steeg and Vastenburg, 2010; Koh et al., 2020). As the penetration depth increases, the cone tip resistance reaches the critical pressure, which is a quasi-stationary value that depends on the density of the sand (Puech and Foray, 2002). The cone-tip resistance profile of M1 shows the critical pressure. The equivalent cone tip resistance was determined as the average of values from 1.5 times the pile diameter above and below the pile tip, as suggested by Bustmante and Gianeselli (1982). Accordingly, the equivalent cone tip resistances of the fill materials in the geotextile tubes were selected at two different depth ranges: 5–35 mm and 50–80 mm. Fig. 6 shows the average cone tip resistance in the geotextile tubes within two different depth ranges. The average cone tip resistances of M3 and M4 containing fine material were smaller than those of M1 and M2 without fine material. Previous studies have shown that the internal strength of a geotextile tube filled without fine material is immediately mobilized, whereas that of a tube filled with fine material gradually increases with elapsed time (Shin and Oh, 2002; Lawson, 2008). Kim et al. (2020) also reported that the unit weight of a geotextile tube filled with fine materials increased over time. The average cone tip resistance of M2 was smaller than that of M1. Notably, M1 had a smaller mean diameter of soil particles but higher unit weight than M2. The results are in good agreement with the findings that cone tip resistance is affected not only by a specific particle size but also by various other factors, such as the coefficient of uniformity and bulk density (Wang et al., 2013; Kim et al., 2019). Regardless of the penetration depth, the average cone tip resistance was greater at L1 than that at L2. The difference in the average cone tip resistances between the locations was owing to the relatively large capacity of the pump for the geotextile tube volume, considering that the ratio of the pump capacity to the volume of the geotextile tube in this study was larger than that reported by Oh and Shin (2006). Shin

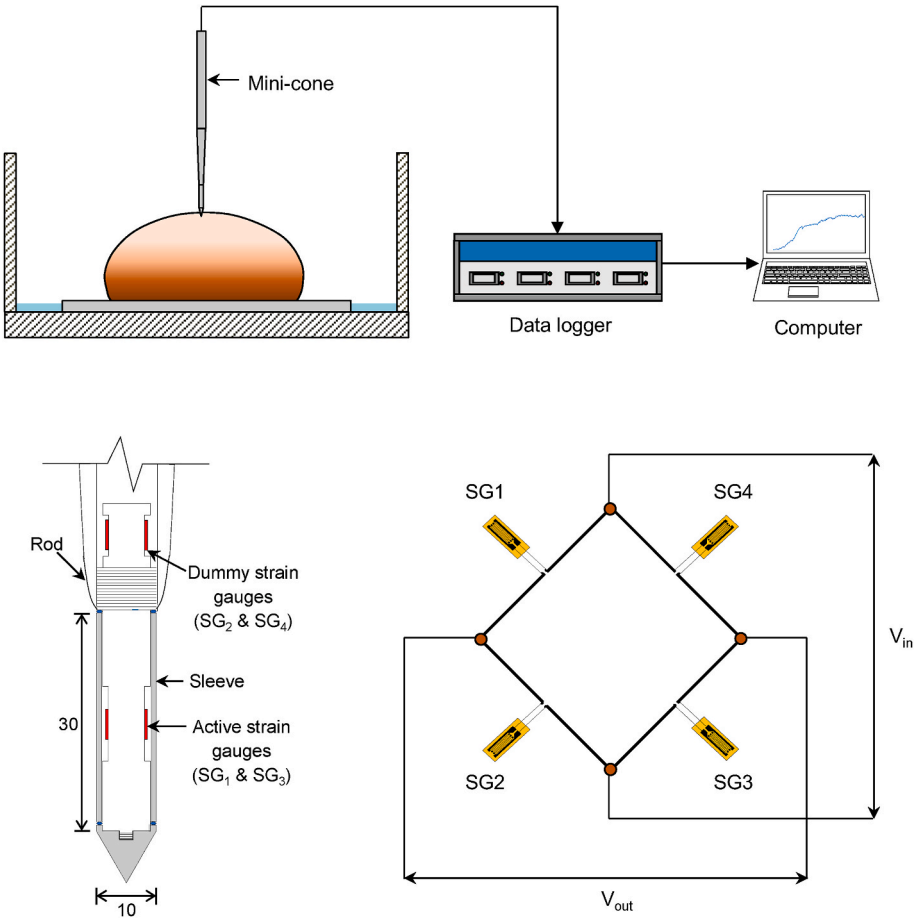

Fig. 4. Miniature cone penetrometer system for internal strength characterization of geotextile tube. The numbers are in the unit of mm.

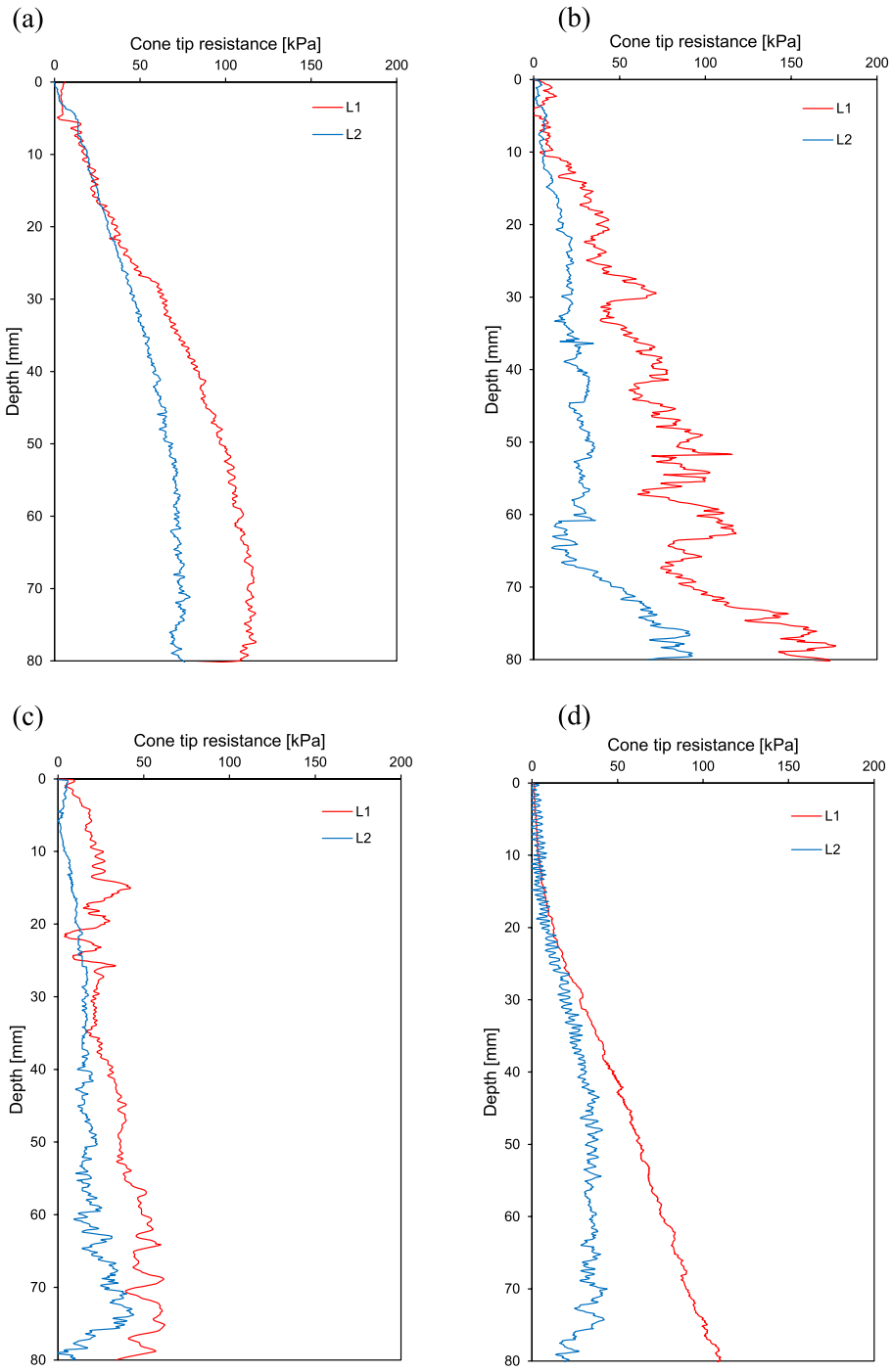

Fig. 5. Profiles of cone tip resistance for geotextile tubes with two different fill materials: (a) M1; (b) M2; (c) M3; (d) M4.

and Oh (2002) reported that the undrained shear strengths in the vicinity of the inlet of the geotextile tube were smaller than those farther from the inlet in the longitudinal direction. Considering that the height of L1 was larger than that of L2 because of the y-shaped pipe splitter, it is likely that the coarser particles of the fill material accumulated first around L1 rather than around L2. Accordingly, for depths of 50–80 mm, the difference in the cone tip resistances between L1 and L2 was significantly greater than that at depths of 5–35 mm. Thus, the strength characterization approach using a miniature cone may be useful for assessing the internal stability of geotextile tubes filled with sandy soils with various particle size distributions.

4. Conclusions

Geotextile tubes have been applied in the coastal engineering field with little consideration for how different materials affect their internal stability. This study investigated the internal shear strength of geotextile tubes using a miniature cone considering the effect of the particle size of the fill material. Four fill materials with different particle size distributions were prepared, and geotextile tubes were filled using a pump. The dewatering time and the height of the geotextile tubes were measured. Cone penetration tests were conducted at the center of the measurement lines using a miniature cone.

The cone tip resistance profiles of the geotextile tubes depended on the particle size distribution of the fill materials and the longitudinal

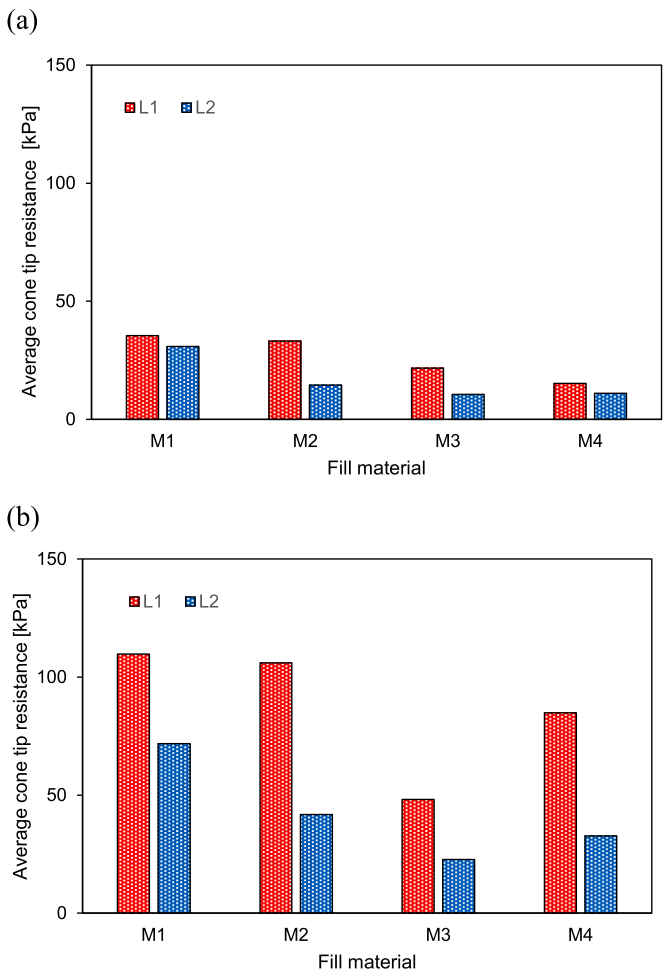

Fig. 6. Average cone tip resistance at two locations for penetration depths of (a) 5–35 mm and (b) 50–80 mm.

location. The poorly graded sand showed the critical pressure in the cone tip resistance profile, while the other materials continued to show some variation in the cone tip resistance profile. Additional cone penetration tests with larger geotextile tubes and extended penetration depth are needed in further studies to investigate the critical pressure for each fill material type. The cone tip resistances of the fill materials with fines content were smaller than those of the fill materials without fine content. The cone tip resistances near the inlet of the geotextile tube were smaller than those far from the inlet in the longitudinal direction. Furthermore, the relationship between the internal strength and material density at each location should be investigated in the near future by measuring the localized volume and weight of the fill material at each location in the geotextile tube. In summary, the strength characterization approach using a miniature cone suggested in this study can be an effective method for assessing the internal stability of geotextile tubes filled with various sandy soils.

CRediT authorship contribution statement

Dong-Ju Kim: Investigation, Data curation, Visualization, Writing – original draft. **Sang-Chul Kim:** Investigation, Data curation. **Jong-Sub Lee:** Conceptualization, Methodology. **Yong-Hoon Byun:** Conceptualization, Methodology, Funding acquisition, Writing – review & editing, Supervision. **Byung-Yoon Kang:** Funding acquisition.

Declaration of competing interest

The authors declare that they have no known competing financial interests or personal relationships that could have appeared to influence the work reported in this paper.

Data availability

The data that has been used is confidential.

Acknowledgements

This work was supported by the National Research Foundation of Korea (NRF) grant funded by the Korean government (MSIT) (No. NRF-2021R1A5A1032433) and Korea Institute of Planning and Evaluation for Technology in Food, Agriculture and Forestry (IPET) through Agricultural Foundation and Disaster Response Technology Development Program, funded by Ministry of Agriculture, Food and Rural Affairs (MAFRA) (320045032HD020).

References

Alvarez, I.E., Rubio, R., Ricalde, H., 2007. Beach restoration with geotextile tubes as submerged breakwaters in Yucatan, Mexico. Geotext. Geomembr 25, 233–241.
Bolton, M.D., Gui, M.W., Garnier, J., Corte, J.F., Bagge, G., Laue, J., Renzi, R., 1999. Centrifuge cone penetration tests in sand. Geotechnique 49, 543–552.
Bustmante, M., Gianeselli, L., 1982. Pile bearing capacity prediction by means of static penetrometer CPT. In: Proceedings of the 2nd European Symposium on Penetration Testing, vol. 2. Balkema, Amsterdam, the Netherlads, pp. 493–500.
Byun, Y.H., Kim, J.H., Lee, J.S., 2013. Cone penetrometer with a helical-type outer screw rod for evaluation of the subgrade condition. J. Transport. Eng. 139, 115–122.
Cantré, S., 2002. Geotextile tubes—analytical design aspects. Geotext. Geomembranes 20, 305–319.
Cho, S.M., Jeon, B.S., Park, S.I., Yoon, H.C., 2008. Geotextile tube application as the cofferdam at the foreshore with large tidal range for Incheon bridge project. In: Geosynthetics Civ. Environ. Eng. Heidelb, pp. 591–596.
Das Neves, L., Moreira, A., Taveira-Pinto, F., Lopes, M.L., Veloso-Gomes, F., 2015. Performance of submerged nearshore sand-filled geosystems for coastal protection. Coast. Eng. 95, 147–159.
Fowler, J., Bagby, R.M., Trainer, E., 1996. Dewatering sewage sludge with geotextile tubes. In: Proceedings of the 49th Canadian Geotechnical Conference. St John's, NLE, Canada, pp. 129–137.
Hirst, T.J., Richars, A.F., Inderbitzen, A.L., 1972. A Static Cone Penetrometer for Ocean Sediments. ASTM International.
ISO 12956, 1999. Geotextiles and Geotextile-Related Products-Determination of the Characteristic Opening Size.
Karadoğan, Ü., Çevikbilen, G., Korkut, S., Pasaoglu, M.E., Teymur, B., 2022. Dewatering of Golden Horn sludge with geotextile tube and determination of optimum operating conditions: a novel approach. Mar. Georesour. Geotechnol. 40, 782–794.
Kim, D.J., Son, D.G., Lee, J.S., Kang, T.H.K., Yun, T.S., Byun, Y.H., 2022. Characterization of Stacked Geotextile Tube Structure Using Digital Image Correlation. The 2022 Structures Congress, Seoul, Korea, 2022.
Kim, H.J., Dinoy, P.R., 2021. Two-dimensional consolidation analysis of geotextile tubes filled with fine-grained material. Geotext. Geomembranes 49, 1149–1164.
Kim, H.J., Dinoy, P.R., Kim, H.S., 2020. Tension force analysis of geotextile tubes by half cross-section test. Geotext. Geomembranes 48, 243–256.
Kim, H.J., Won, M.S., Lee, K.H., Jamin, J.C., 2016a. Model tests on dredged soil-filled geocontainers used as containment dikes for the Saemangeum reclamation project in South Korea. Int. J. GeoMech. 16, 04015055.
Kim, H.J., Won, M.S., Jamin, J.C., Joo, J.H., 2016b. Numerical and field test verifications for the deformation behavior of geotextile tubes considering 1D and areal strain. Geotext. Geomembranes 44, 209–218.
Kim, R., Lee, W., Lee, J.S., 2010. Temperature-compensated cone penetration test mini-cone using fiber optic sensors. Geotech. Test J. 33, 243–252.
Kim, S.Y., Hong, W.T., Lee, J.S., 2019. Role of the coefficient of uniformity on the California bearing ratio, penetration resistance, and small strain stiffness of coarse arctic soils. Cold Reg. Sci. Technol. 160, 230–241.
Koerner, G.R., Koerner, R.M., 2006. Geotextile tube assessment using a hanging bag test. Geotext. Geomembranes 24, 129–137.
Koh, J.W., Chew, S.H., Chua, K.E., Yim, H.M.A., Gng, Z.X., 2020. Effect of construction sequence on the performance of geotextile tubes in a containment bund. Int. J. Geom. 19, 1–7.
Khachan, M.M., Bhatia, S.K., 2016. Influence of fibers on the shear strength and dewatering performance of geotextile tubes. Geosynth. Int. 23, 317–330.
Lawson, C.R., 2008. Geotextile containment for hydraulic and environmental engineering. Geosynth. Int. 15, 384–427.
Leshchinsky, D., Leshchinsky, O., Ling, H.I., Gilbert, P.A., 1996. Geosynthetic tubes for confining pressurized slurry: some design aspects. J. Geotech. Eng. 122, 682–690.

Lee, W., Shin, D.H., Yoon, H.K., Lee, J.S., 2009. Micro-cone penetrometer for more concise subsurface layer detection. Geotech. Test J. 32, 358–364.
Man, X.L., Shu, Y.M., Yu, C.L., Hao, X.H., Li, S.P., 2018. Effect of cyclic wave loading on scouring stability of geotube dams. Ocean Eng. 152, 1–5.
McCafferty, C., Hsuan, G., 2020. Analyzing filtration flow rate change of woven geotextiles for fine grained slurries. Geosynth. Int. 27, 655–661.
Moo-Young, H.K., Tucker, W.R., 2002. Evaluation of vacuum filtration testing for geotextile tubes. Geotext. Geomembranes 20, 191–212.
Oh, Y.I., Shin, E.C., 2006. Using submerged geotextile tubes in the protection of the E. Korean shore. Coast. Eng. 53, 879–895.
Palmeira, E.M., Melo, D.L.A., Moraes-Filho, I.P., 2019. Geotextile filtration opening size under tension and confinement. Geotext. Geomembranes 47, 566–576.
Puech, A., Foray, P., 2002. Refined model for interpreting shallow penetration CPTs in sands. In: Offshore Technology Conference. OnePetro.
Shin, E.C., Kang, J.K., Kim, S.H., Park, J.J., 2016. Construction technology of environmental sustainable shore and harbor structures using stacked geotextile tube. KSCE J. Civ. Eng. 20, 2095–2102.
Shin, E.C., Oh, Y.I., 2002. Installation technology and behavior of silty clay filled geotextile tube. J. Korean Geosynth Soc. 1, 13–21.
Shin, E.C., Oh, Y.I., 2003. Analysis of geotextile tube behaviour by large-scale field model tests. Geosynth. Int. 10, 134–141.
Shin, E.C., Oh, Y.I., 2007. Coastal erosion prevention by geotextile tube technology. Geotext. Geomembranes 25, 264–277.
Tumay, M.T., Kurup, P.U., 2001. Development of a continuous intrusion miniature cone penetration test system for subsurface explorations. Soils Found. 41, 129–138.
Van Steeg, P., Vastenburg, E.W., 2010. Large Scale Physical Model Tests on the Stability of Geotextile Tubes. Deltares Report 1200162-000.
Wang, J.J., Zhang, H.P., Tang, S.C., Liang, Y., 2013. Effects of particle size distribution on shear strength of accumulation soil. J. Geotech. Geoenviron. Eng. 139, 1994–1997.
Yang, J., 2006. Influence zone for end bearing of piles in sand. J. Geotech. Geoenviron. Eng. 132 (9), 1229–1237.
Yee, T.W., Lawson, C.R., 2012. Modelling the geotextile tube dewatering process. Geosynth. Int. 19, 339–353.
Yoon, H.K., Truong, Q.H., Byun, Y.H., Lee, J.S., 2015. Capillary effect in salt-cemented media of particle sizes. J. Appl. Geophys. 112, 20–28.
Yoon, H.K., Lee, J.S., 2012. Microcones configured with full-bridge circuits. Soil Dyn. Earthquake Eng. Elsevier. 41, 119–127.